



**HAL**  
open science

## High sensitivity capillary electrophoresis with fluorescent detection for glycan mapping

Théo Liénard–Mayor, Bin Yang, Nguyet Thuy Tran, Arnaud Bruneel, Andras Guttman, Myriam Taverna, Thanh Duc Mai

► **To cite this version:**

Théo Liénard–Mayor, Bin Yang, Nguyet Thuy Tran, Arnaud Bruneel, Andras Guttman, et al.. High sensitivity capillary electrophoresis with fluorescent detection for glycan mapping. *Journal of Chromatography A*, 2021, 1657, pp.462593. 10.1016/j.chroma.2021.462593 . hal-04259361

**HAL Id: hal-04259361**

**<https://universite-paris-saclay.hal.science/hal-04259361>**

Submitted on 22 Jul 2024

**HAL** is a multi-disciplinary open access archive for the deposit and dissemination of scientific research documents, whether they are published or not. The documents may come from teaching and research institutions in France or abroad, or from public or private research centers.

L'archive ouverte pluridisciplinaire **HAL**, est destinée au dépôt et à la diffusion de documents scientifiques de niveau recherche, publiés ou non, émanant des établissements d'enseignement et de recherche français ou étrangers, des laboratoires publics ou privés.



Distributed under a Creative Commons Attribution - NonCommercial 4.0 International License

1 **High sensitivity capillary electrophoresis with fluorescent detection for glycan mapping**

2

3 **Théo Liénard--Mayor<sup>1</sup>, Bin Yang<sup>1</sup>, Nguyet Thuy Tran<sup>1</sup>, Arnaud Bruneel<sup>2,3</sup>, Andras**

4 **Guttman<sup>4,5</sup>, Myriam Taverna<sup>1,6</sup>, Thanh Duc Mai<sup>1\*</sup>**

5

6 *<sup>1</sup> Institut Galien Paris Sud, UMR 8612, Protein and Nanotechnology in Analytical Science*

7 *(PNAS), CNRS, Univ. Paris-Sud, Univ. Paris-Saclay, 5 rue Jean Baptiste Clément, 92290*

8 *Châtenay-Malabry, France*

9 *<sup>2</sup> Université Paris-Saclay, INSERM UMR1193, Mécanismes cellulaires et moléculaires de*

10 *l'adaptation au stress et cancérogenèse, Châtenay-Malabry, France*

11 *<sup>3</sup> AP-HP, Biochimie Métabolique et Cellulaire, Hôpital Bichat-Claude Bernard, Paris, France*

12 *<sup>4</sup> Translational Glycomics Research Group, Research Institute of Biomolecular and Chemical*

13 *Engineering, University of Pannonia, 10 Egyetem Street, Veszprem 8200, Hungary*

14 *<sup>5</sup> Horváth Csaba Laboratory of Bioseparation Sciences, Research Centre for Molecular*

15 *Medicine, Faculty of Medicine, University of Debrecen, 98 Nagyerdei Krt, Debrecen*

16 *4032, Hungary*

17 *<sup>6</sup> Institut Universitaire de France (IUF)*

18

19 \* Corresponding author

20 e-mails: [thanh-duc.mai@u-psud.fr](mailto:thanh-duc.mai@u-psud.fr)

21

22 **Keywords:** background electrolyte; capillary electrophoresis; fluorescent detection; large

23 volume sample stacking; N-glycans

24

25

26 **Abstract**

27 We present in this study a novel strategy to drastically improve the detection sensitivity and  
28 peak capacity for capillary electrophoresis with laser induced fluorescent detection (CE-LIF)  
29 of glucose oligomers and released glycans. This is based on a new approach exploiting a  
30 polymer-free background electrolyte (BGE) for CE-LIF of glycans. The best performance in  
31 terms of sample stacking and suppression of electroosmotic flow (EOF) was found for a BGE  
32 composed of triethanolamine / citric acid and triethanolamine / acetic acid at elevated ionic  
33 strengths (IS up to 200 mM). Compared to the conventional protocols for CE-LIF of glucose-  
34 oligosaccharides and released glycans, our polymer-free strategy offered up to 5-fold  
35 improvement of detection sensitivity and visualization of higher degree of polymerization  
36 (DP) of glucose oligomers (18 vs 15). To further improve the detection sensitivity, a new  
37 electrokinetic preconcentration strategy via large volume sample stacking with electroosmotic  
38 modulation without having recourse to neutrally coated capillaries is proposed, offering a 200-  
39 fold signal enhancement. This approach is based on variation of the buffer's IS, rather than pH  
40 adjustment as in conventional methods, for EOF modulation or quasi-total reduction. This  
41 strategy allows selecting with high flexibility the best pH conditions to perform efficient  
42 preconcentration and separation. The new approach was demonstrated to be applicable for the  
43 analysis of N-linked oligosaccharides released from a model glycoprotein (Human  
44 Immunoglobulin G ) and applied to map N-glycans from human serum for congenital  
45 disorders of glycosylation (CDG) diagnosis.

46

47

48 **1. Introduction**

49 Analysis of glycans released from glycoproteins plays an important role for quality control of  
50 therapeutic proteins and diagnostic purposes [1, 2]. Protein glycosylation is by far the most  
51 complex common post-translational modification, with more than half of all secretory and  
52 cellular proteins being glycosylated [3-5]. An altered glycosidic linkage or one truncated  
53 antenna in a glycan may alter the normal functioning and activity of glycoproteins. A  
54 variation of glycoform proportion of a given glycoprotein may also have biological  
55 consequences or be the result of a pathological state [6]. That is why glycoproteins represent a  
56 useful source of biomarkers for various illnesses like cancer and cardiovascular diseases [2].  
57 Another typical example is congenital disorders of glycosylation (CDG), a family of  
58 multisystem genetic diseases caused by mutations in genes coding for proteins involved in the  
59 biosynthesis (CDG-I) or trimming/remodeling (CDG-II) of the oligosaccharide moieties of N-  
60 linked glycoconjugates [7]. Thus, CDG-I leaves some N-glycosylation sites unoccupied while  
61 CDG-II is associated with subtle structural changes of N-glycans with a whole array of  
62 isomers, leading to a great challenge for their separation and identification.

63  
64 Until now, analysis of glycans have frequently been carried out with high-performance liquid  
65 chromatography with fluorescence detection (HPLC-FLD) [8], matrix-assisted laser  
66 desorption/ ionization time-of-flight mass spectrometry (MALDI-TOF-MS) [9, 10], or liquid  
67 chromatography connected to electrospray ionization mass spectrometry (LC-ESI-MS) [7].  
68 Capillary electrophoresis (CE) coupled with laser induced fluorescent (LIF) detection has  
69 become a staple in glycan separation, mostly for N-glycans [11, 12]. Prior to downstream  
70 analysis, sample preparation is required, especially when performing sensitive detection is the  
71 objective [13]. It stands for both small compounds and large biomolecules. In a standard  
72 protocol for glycans, glycans are first released from glycoproteins / peptides, enriched on a

73 solid support (i.e., magnetic beads in most of the cases), then fluorescently labelled with a  
74 charged fluorophore (the most frequently used one being 8-aminopyrene-1,3,6-trisulfonic-acid  
75 (APTS) [14]) and eventually separated by CE-LIF. Normally, acidic background electrolytes  
76 (BGEs) containing different polymer/gel types and concentrations, typically polyethylene  
77 oxide (PEO) or polyethylene glycol (PEG), are used [15]. The CE-LIF conditions for glycan  
78 analysis have recently been established with the introduction of commercial kits, including  
79 polymer-containing buffers [16, 17]. Efforts to use gel-free BGEs for such purpose were also  
80 reported in the early 90's [18-20], but were then outnumbered by those that use gels and  
81 polymers in recent years.

82

83 So far, reported BGE compositions for CE-LIF of glycans normally employ inorganic and  
84 small ions (*e.g.*, phosphate, borate, acetate, sodium, lithium) as well as inorganic acid and  
85 base (typically NaOH and HCl) for pH adjustment. From our viewpoint, such BGEs with low  
86 UV absorbing features are adapted for UV detection but the significant increase in their ionic  
87 strengths, which is required for improving analyte stacking and suppressing further the  
88 electroosmotic flow (EOF), is not trivial to achieve due to detrimental increase in electric  
89 currents and thus Joule heating. To further increase the detection sensitivity and peak  
90 capacity, the challenge is to find a BGE that simultaneously satisfies the criteria of efficient  
91 sample stacking (for increased glycans' signals), EOF suppression (for migration of large  
92 glycans counter the EOF to the detector) and tolerable current generation. A straightforward,  
93 cost-effective and coating-free CE-LIF approach that offers such features for glycan  
94 separation is therefore highly desirable. In the diagnostic context, there are still challenges for  
95 the detection of glycans used as biomarkers, mostly due to the low abundance of some plasma  
96 glycoproteins and unsatisfactory detection sensitivity. This therefore requires continued  
97 development to improve the CE-LIF performance towards the screening/diagnosis of

98 aberrant-glycan-related pathologies. Efforts have been focused on glycan sample treatment  
99 (fluorescent labeling [21-23]) and glycan enrichment methods based on solid phase extraction  
100 [24, 25] or electrokinetic phenomena (notably isotachopheresis and large volume sample  
101 stacking) [26-29] prior to CE-LIF.

102  
103 In this study, we report a novel strategy to significantly improve the performance of CE-LIF  
104 of fluorescently labelled glycans, using polymer-free buffers in conjunction with efficient  
105 analyte stacking and EOF suppression in fused silica capillaries. To demonstrate the  
106 applicability of our new approach, CE-LIF analyses of N-glycans released from a model  
107 glycoprotein (Human Immunoglobulin G ) were carried out and the performance in terms of  
108 signal sensitivity and peak capacity was compared to currently used methods. The developed  
109 approach was applied for mapping of N-glycans released from human serum glycoproteins,  
110 serving for CDG screening.

111

## 112 **2. Experimental**

### 113 **2.1. Chemicals, reagents and samples**

114 All chemicals for preparation of buffers were of analytical or reagent grade and purchased  
115 from Sigma-Aldrich (Lyon, France). Reagents for preparation of glycans (denaturation,  
116 digestion, labeling solutions; malto-oligosaccharides (MD ladder), APTS dye, magnetic beads  
117 and G3 standard) were taken from the Fast Glycan Analysis and Labeling kit from SCIEX  
118 (Villebon sur Yvette, France). Human Immunoglobulin G (IgG), PNGase F and sodium  
119 cyanoborohydride ( $\text{NaBH}_3\text{CN}$ ) were purchased from Sigma-Aldrich (Lyon, France). Maltose  
120 (G2) was obtained from Sigma-Aldrich and Maltohexose (G6) was obtained from Carbosynth  
121 Limited (Compton, UK). Beta-alanine ( $\beta$ -Ala), triethanolamine (TEOA), trimellitic acid,  
122 acetic acid (AcOH), citric acid (Cit) and lithium hydroxide monohydrate were used for

123 preparation of BGE solutions. Serum samples from CDG individuals and healthy control were  
124 kindly provided by Dr. A. Bruneel (Bichat hospital, Paris, France).

125

## 126 **2.2. Apparatus and Material**

127 Method development was performed with a Beckman Coulter PA800+ and MDQ systems  
128 (SCIEX, Brea, CA) coupled with a LIF detector ( $\lambda_{\text{excitation}}$ : 488 nm,  $\lambda_{\text{emission}}$ : 520 nm).

129 Instrument control and data acquisition were carried out by using the 32Karat ver 8.0 software  
130 (SCIEX). Fused silica capillaries of 50  $\mu\text{m}$  i.d. and 375  $\mu\text{m}$  o.d. from Polymicro (TSP050375,

131 CM Scientific, Silsden, UK) were used for all CE experiments. Deionized water was purified  
132 using a Direct-Q3 UV purification system (Millipore, Milford, MA, USA) and the pH values

133 of buffer solutions and samples were measured with a SevenCompact pH meter (Mettler

134 Toledo, Schwerzenbach, Switzerland). Buffer ionic strength (IS) calculations were based on

135 simulations with the computer program PhoeBus (Analis, Suarlée, Belgium). Additional

136 information regarding the simulation by Phoebus program can be found in reference [30]. To

137 maximize the accuracy for a defined buffer's ionic strength, calculation was implemented

138 with correction according to either Debye-Hückel equation (ionic strengths of 1-10 mmol/L),

139 Güntelberg equation (ionic strengths of 10-60 mmol/L) or Davies equation (ionic strengths of

140 60-500 mmol/L). Deionized water was used for the preparation of all solutions.

141

## 142 **2.3. Methods**

### 143 *2.3.1. Release and fluorescent labelling of glycoprotein derived-glycans*

144 10  $\mu\text{L}$  of human IgG (10 mg/mL in deionized water) was mixed with 5  $\mu\text{L}$  of the denaturing  
145 solution containing 10  $\mu\text{L}$  of D1 solution, 10  $\mu\text{L}$  of D3 solution and 50  $\mu\text{L}$  of D4 solution

146 from the SCIEX kit and incubated at 70°C for 10 min. After denaturation, 12  $\mu\text{L}$  of the

147 digestion solution containing 5  $\mu\text{L}$  of PNGase F in 12  $\mu\text{L}$  of D4 was added and further

148 incubated for 60 minutes at 50°C. The released glycans were then labelled following the  
149 protocol described in [22]. Briefly, labelling reagents (3 µL of 40 mM APTS in 20% AcOH, 2  
150 µL of 1 M NaBH<sub>3</sub>CN) in THF, 4 µL of 20% AcOH and 6 µL of THF) were added into the  
151 sample vial and incubated for 60 min at 50°C with closed cap, and then for 60 min at 50°C via  
152 evaporative labelling with open cap.

153  
154 For the preparation of N-glycans from human serum samples, the magnetic beads delivered in  
155 the SCIEX kit were used for sample purification. The tube containing 200 µL of resuspended  
156 magnetic beads was placed in a magnetic stand to allow the beads migrating to the magnet,  
157 then the storage buffer was removed. This step was performed every time to remove any  
158 liquid from the beads. 10 µL of 4-fold diluted serum sample was added onto the beads. 5 µL  
159 of denaturing solution was then added, mixed and incubated at room temperature for 7 min  
160 with the vial opened. 11 µL of digestion solution from Sciex kit was added to the mixture; and  
161 incubated at 60°C for 20 min in an open vial. 200 µL of acetonitrile was then added, mixed  
162 and incubated at room temperature for 1 min. The supernatant was removed, and 9 µL of 40  
163 mM APTS in 20% acetic acid, 1 µL of NaCNBH<sub>3</sub> and 1 µL of D4 from the SCIEX kit was  
164 added, followed by incubation at 60 °C for 20 min in an open vial.

165  
166 *2.3.2. Fluorescent labelling of standard oligosaccharides*

167 The preparation of fluorescently labelled *MD* ladders was performed according to Reider *et*  
168 *al.* [22]. Briefly, 2 mg of oligosaccharide ladder was added in a 200 µL PCR tube, followed  
169 by addition of 4 µL of 40 mM APTS in 20% AcOH, 4 µL of 20% AcOH and 2 µL of 1M  
170 sodium cyanoborohydride (NaBH<sub>3</sub>CN) in tetrahydrofuran (THF). The mixture was incubated  
171 under mixing at 70°C for 30 min with an open-capped vial. After the reaction, the sample was

172 stocked in 100  $\mu$ L deionized water, which was aliquoted and stored at  $-20^{\circ}\text{C}$ . Further dilution  
173 of this stock solution was carried out before CE-LIF analysis.

174

### 175 *2.3.3. CE-LIF of APTS-glycans and oligosaccharides*

176 Analyses of the APTS-labeled N-glycans or the malto-oligosaccharide standards were carried  
177 out either with various BGEs detailed in Table 1 or using the SCIEX gel buffer system (BGE  
178 SCIEX). These separations were done using fused-silica capillaries of 50  $\mu\text{m}$  i.d. with the  
179 total length ( $L_{\text{tot}}$ ) of 60 cm, the effective length ( $L_{\text{eff}}$ ) of 50 cm, under a separation voltage of -  
180 25 kV applied on the injection (inlet) side . The fused silica capillaries were preconditioned by  
181 rinsing with 0.1 M NaOH for 5 min, water for 3 min and the buffer of interest for 10 min prior  
182 to use.

183

184 Large-volume sample stacking with EOF modulation was implemented with BGE composed  
185 of TEOA / citric acid (IS of 150 mM, pH 4.75). The sample prepared in water was  
186 hydrodynamically filled to 100 % of the capillary volume (0.7 psi, 900 sec). A voltage of -  
187 25kV was applied on the injection (inlet) side to stack the target oligosaccharides / glycans.  
188 The preconcentration step was transitioned into the separation step without user intervention  
189 when the current stopped increase and reached a stable value.

190

## 191 **3. Results and Discussion**

### 192 **3.1. Polymer-free BGEs for CE-LIF of APTS-labeled malto-oligosaccharides and** 193 **glycans**

#### 194 *3.1.1. Proposed principle*

195 Our proposed approach, illustrated in Fig. 1A, is to push the ionic strengths (IS) of the BGE  
196 and concentrations to extremely high levels (IS up to 200 mM, which require concentrations

197 up to a thousand mM) to allow high stacking of APTS-labelled glycans induced by the  
198 conductivity differences between the sample and buffer zones [31, 32]. At the same time,  
199 these conditions ensure suppression of EOF without recourse to any capillary coating via  
200 diminution of the electrical double layer thickness on the internal capillary surface [33, 34],  
201 while still maintaining tolerable electric currents. This EOF suppression is desirable to allow  
202 the anionic labeled glycans to migrate towards the detector. Whereas this was difficult with  
203 buffers containing inorganic ions, we expected it to be realizable with BGEs composed of  
204 large weakly charged molecules with low degrees of protonation / ionization. These molecules  
205 have indeed been used for preparation of BGEs for CE coupled with contactless conductivity  
206 detection. Their concentrations in this case are normally kept low (less than 50 mM in  
207 general) in order to minimize the generated background signal [31, 35]. In our study, we  
208 targeted much higher buffer concentration ranges (up to a thousand mM) than typically  
209 reported. As the electric currents are directly related to the conductivity, which in turns links  
210 to the ion density of the BGE (*i.e.*, IS) and ions' electrophoretic mobilities ( $\mu_{ep}$ ), the very-  
211 slowly-migrating ions (ideally,  $\mu_{ep}$  approaching zero) were anticipated to provide much lower  
212 currents than the conventional BGE constituents, even at very high IS and concentrations.

213

### 214 **3.1.2. Performance of the polymer-free BGEs**

215 To follow the logic described above, several BGEs that were designed by simulation using the  
216 Phoebus software to meet the aforementioned criteria were selected (Table 1). Four BGE  
217 candidates from the simulated ones were experimentally tested, including TEOA/ citric acid,  
218 TEOA / acetic acid,  $\beta$ -Ala / acetic acid and  $\beta$ -Ala / trimellitic acid. The EO mobilities  
219 obtained with these BGEs, measured using the method developed by Williams et Vigh [36],  
220 were  $0.47 \times 10^{-5} \text{ cm}^2 \cdot \text{V}^{-1} \cdot \text{s}^{-1}$  for TEOA/ citric acid,  $1.28 \times 10^{-5} \text{ cm}^2 \cdot \text{V}^{-1} \cdot \text{s}^{-1}$  for TEOA / acetic  
221 acid,  $4.82 \times 10^{-5} \text{ cm}^2 \cdot \text{V}^{-1} \cdot \text{s}^{-1}$  for  $\beta$ -Ala / acetic acid and  $4,72 \times 10^{-5} \text{ cm}^2 \cdot \text{V}^{-1} \cdot \text{s}^{-1}$  for  $\beta$ -Ala /

222 trimellitic acid buffer, respectively. The EO mobility was reduced by up to 10 folds when  
223 using TEOA-based BGEs instead of  $\beta$ -Ala-based ones. Note that the EO mobilities achieved  
224 with neutral coatings are normally inferior to  $1 \times 10^{-5} \text{ cm}^2 \cdot \text{V}^{-1} \cdot \text{s}^{-1}$  [37, 38]. These BGEs were  
225 used for the separation of the APTS-labeled MD ladder, and the performance was evaluated in  
226 terms of peak intensity and capacity. The lithium acetate buffer (LiOH/AcOH), a polymer-  
227 free BGE employed by many groups for CE-LIF of oligosaccharides [11, 15], was also tested  
228 as a reference. The others in the list (e.g., TEOA / gluconic acid, TEOA / sorbic acid, etc.)  
229 were not tested due to limited solubilities of the least soluble components in these buffers.  
230 Performance comparison for CE-LIF of the APTS-labelled oligosaccharide ladder with the 5  
231 investigated BGEs is shown in Fig. 2. As can be seen, peak signals achieved with our 4  
232 proposed BGEs (Fig. 2B-E) are all significantly higher than those obtained with LiOH/AcOH  
233 buffer (Fig. 2A). Particularly, the peak heights obtained with TEOA/Cit and TEOA/AcOH  
234 were up to 5-fold higher than those obtained with LiOH/AcOH BGE. Furthermore, the  
235 TEOA-based buffers could suppress EOF more efficiently, allowing detection of longer  
236 glucose oligomers, up to 12 and 17 glucose units (DP) for TEOA/AcOH (Fig. 2D) and  
237 TEOA/Cit (Fig. 2E), respectively, whereas only 6 DP peaks are found with LiOH/AcOH  
238 under the same CE conditions. In the case of 150 mM  $\beta$ -Ala/Trimellitic acid (Fig. 2B) and  
239 150 mM  $\beta$ -Ala / AcOH (Fig. 2C), one can see that the signals were also approximately 5-fold  
240 higher than those from the reference LiOH/AcOH. The number of observed malto-  
241 oligosaccharides was, however, much lower than that for TEOA based buffers. The best  
242 performance in terms of peak heights and detected DP number was achieved with  
243 TEOA/AcOH and TEOA/Cit buffers. Table 2 further shows that the signal to noise ratios  
244 were approximately 10-times higher with TEOA-based buffers compared to the standard  
245 LiOH/AcOH one. Satisfactory repeatability for migration times (RSD % < 0.5 %) and peak  
246 areas (RSD < 5 %) was achieved for the investigated peaks with these buffers (Table 2). The

247 overall results clearly show the superiority of TEOA/Cit BGE. The improved signals observed  
248 with our buffers are probably linked to the prolonged duration ( $\Delta t$ ) to maintain the stacking  
249 effect. Indeed, good sample stacking in CE is not only dependent on the conductivity  
250 difference ( $\Delta\sigma$ ) between the sample and electrolyte zones (similar to optimization of  
251 conductivity signals [31]), but also on the duration ( $\Delta t$ ) to maintain such difference. With  
252 conventional BGE, the initial  $\Delta\sigma$  is normally satisfied (*via* high  $\mu_{ep}$  at low and moderate IS) at  
253 the starting moment, however, decreases when the fast-moving ions in the BGE zone  
254 penetrate into the sample zone (Kohlrausch regulating function [39, 40]). This stacking effect  
255 is on the other hand expected to reach the maximum for extremely concentrated slowly  
256 migrating BGE ions (see Fig. 1A), thanks to high  $\Delta\sigma$  (*via* very high IS even with low  $\mu_{ep}$ ) and  
257 longer  $\Delta t$  (due to retardation of the ion penetration from the BGE into the sample zone).  
258 Furthermore, by using an extremely dense zone of large weakly charged ions in the BGE, the  
259 diffusion of stacked analytes may be hindered by the clusters or groups of electrolyte  
260 molecules [41]. This in turn can help “blocking” the stacked analytes more efficiently at the  
261 sample-BGE boundary for further peak height improvement.

262  
263 The IS of this BGE was then further increased in order to achieve greater stacking effect, and  
264 thus gaining further improvement of peak signals for the APTS-labeled MD ladder (Fig 3).  
265 Oligosaccharide peaks obtained with TEOA/Cit BGE at IS of 200 mM were slightly higher  
266 (1.3 - 1.5x improvement) compared to those obtained with 150 mM IS. Interestingly, the EOF  
267 was slightly higher with the 200 mM BGE with some retardation of the oligosaccharide peaks,  
268 which was probably due to some increase in pH. Indeed, when working with very  
269 concentrated solutions, their experimentally measured pH values were found slightly shifted  
270 from the simulated ones. In the case of TEOA/Cit BGE at IS of 200 mM, the measured pH  
271 was 5.05 instead of 4.75 as simulated. This can refer to a similar situation when measuring the

272 pH values of very salty solutions, where the aqueous proton ( $H^+$ ) concentration is different  
273 from its activity, leading to a shift of pH value that reflects the solution  $H^+$  activity.  
274 Consequently, fewer malto-oligosaccharide peaks (15 DPs) were observed in that case over 20  
275 min. Thus, IS can be selected between 150 or 200 mM depending whether a higher number of  
276 detected malto-oligosaccharides is required. The variation of MD ladders' signals at lower IS  
277 ranges was also verified for the TEOA / Cit BGE (Fig S1 in the ESI). The signals approached  
278 the plateau at IS from 100 mM; and the increase in peaks' signals was less significant between  
279 100 - 200 mM. The use of high IS (150 or 200 mM rather than 100 mM or less) is indeed not  
280 only for signal improvement, but also for efficient EOF suppression to facilitate the migration  
281 of glycans to the detector. IS higher than 200 mM was as well tested but then was not  
282 considered for further experiments due to too high currents (more than  $65 \mu A$ , which can  
283 generate pronounced Joule heating for a capillary of  $50 \mu m$  i.d.). The TEOA/Cit BGE was  
284 also compared with the commercial one (SCIEX polymer containing BGE) for successive  
285 separations of oligosaccharides (over 15 runs). Peak heights were almost 4-fold higher for  
286 TEOA/Cit 200 mM (Fig. 3B) compared to those obtained with the commercial buffer (Fig.  
287 3C). The TEOA/Cit BGE exhibited similar repeatability of migration times ( $RSD \% < 0.8 \%$   
288 over 15 runs for DP 1, DP 6 and DP 10 oligomers, (table S1 in the supplementary material) as  
289 with the commercial buffer. Better peak capacity was achieved for TEOA/Cit polymer-free  
290 buffers. This advantageous feature can be explained by several features. First, thanks to the  
291 drastic reduction of the zeta potential of the inner capillary surface at very high IS of the  
292 buffer, significant EOF suppression could be obtained [33, 34]. Second, the efficiency of  
293 alkylamines in BGEs for capillary surface coverage via electrostatic interaction with the  
294 ionized silanols of the capillary was higher than that offered by monovalent cations ( $Na^+$ ,  $Li^+$ ,  
295  $K^+$ ,  $NH_4^+$ ) in conventional BGEs [42]. Third, when using very high concentrations of BGE  
296 constituents (approaching their saturation), it is assumed that the solvation degree of the

297 silanol groups of the capillary was decreased due to competition with other ions in the  
298 electrolytes for hydration. The presence of very concentrated ions in our BGEs, thus, could  
299 allow coverage and reduction of the capillary surface charge, decreasing its zeta potential,  
300 which in turn gives a similar effect as a ‘virtual coating’ for EOF suppression.

301

302 ***3.1.3. Analysis of human serum glycans from CDG individuals: towards diagnostic***  
303 ***applications***

304 For CDG screening via N-glycan analysis, the preferred methods include gel electrophoresis,  
305 chromatography and mass spectrometry (MALDI-MS and ESI-MS), whereas CE-LIF has not  
306 been listed yet as a well-established method for this purpose [7]. In order to showcase the  
307 applicability of our new CE-LIF method for the CDG diagnostics, total N-glycans from two  
308 serum samples from CDG patients and one from a healthy person (control) were analyzed by  
309 CE-LIF (Fig. 4). Trace (A) corresponds to the control serum, featuring different peaks from  
310 biantennated N-glycans (peaks a-b-c). Trace (B) shows the serum glycan profile from a  
311 B4GALT1-CDG individual with a quasi-total deficit of galactosylated N-glycans, which  
312 differs significantly from the control one. Trace (C) corresponds to a MGAT2-CDG case,  
313 where one of the N-glycan antennae presents a major GlcNAcylation defect. An extra peak  
314 (peak g at ~11.5 min) that is not present in the control sample was found for this CDG  
315 subtype. Accordingly, very typical and distinct profiles are obtained for the different CDG  
316 subtypes showing that an adequate diagnosis could be possible with N-glycan profiling by  
317 CE-LIF. The peak patterns obtained with our polymer-free BGE were similar to those  
318 obtained with the commercial buffer (Fig. S2 in the supporting material), demonstrating the  
319 applicability of our approach for the analysis of glycans from biofluids. In both CE-LIF  
320 profiles (Fig. 4) and MALDI-MS reference ones [43], featured peaks were found for CDG  
321 samples whereas they were non-detectable in the healthy control. It is worthy to note that

322 unlike CE-LIF, no separation step was carried out prior to ionization for MALDI-MS. The  
323 MS profiles therefore may present some overlaps of glycans having the same mass to charge  
324 ratio and / or presenting poor signals for those hardly ionizable.

325

## 326 **3.2. Large volume sample stacking with EOF modulation in uncoated capillaries**

### 327 ***3.2.1. Proposed principle***

328 In conventional methods of large volume sample stacking with electroosmotic pumping  
329 (LVSEP), which is the most frequently reported approach for electrokinetic preconcentration  
330 of glycans, the EOF variation and suppression is established through buffer pH adjustment  
331 and the use of neutral capillary coatings [26-29, 37, 44]. Unfortunately, such mode of  
332 preconcentration often leads to fast deterioration of the permanent neutral coating layer over  
333 runs [37]. Therefore, we took advantage of our new BGE to develop an analyte  
334 preconcentration approach without recourse to any capillary coating via large volume sample  
335 stacking (LVSS) with EOF modulation (see Fig. 1B). This electrokinetic preconcentration  
336 required indeed two completely different EOF magnitudes for sample preconcentration and  
337 for the separation of the stacked analytes. High electroosmotic mobility (for example  $\mu_{EO} =$   
338  $60 \times 10^{-5} \text{ cm}^2/\text{V/s}$  if the sample is prepared in water) was needed to remove the sample matrix  
339 from the capillary during the stacking of negatively charged analytes, whereas a much lower  
340 one ( $\mu_{EO} \sim 0$ ) was required to ensure the electromigration of enriched glycans to achieve their  
341 baseline separation. Here we propose to use variation of the IS of the BGE, rather than the  
342 buffer pH (not the pH of the sample matrix) as in conventional approach for modulation and  
343 quasi-total reduction of the EOF.

344

### 345 ***3.2.2. Procedure optimization and performance***

346 The challenging part of this approach was to establish in the same uncoated capillary two  
347 distinct EOF ranges that transiently switch from one to another. The very high  $\mu_{\text{EO}}$  (more than  
348  $55 \times 10^{-5} \text{ cm}^2 \cdot \text{V}^{-1} \cdot \text{s}^{-1}$ ) could in principle be obtained by using either water or very diluted  
349 BGE as the sample matrix to be filled in the capillary before the preconcentration step. Our  
350 preliminary optimizations revealed that oligosaccharides prepared in water exhibited the best  
351 EOF-assisted stacking performance. Note that if the sample was prepared in deionized water,  
352 the very low ion density in the sample matrix could sometimes provoke drop of the current  
353 profile during the large volume sample stacking, leading to failure of this preconcentration  
354 step. This challenge was overcome (or at least alleviated) by replacing deionized water with  
355 tap water to ensure a sufficient ion density in the sample matrix. Then, to reach a very low  
356 EOF ( $\mu_{\text{EO}}$  approaching zero) required for CE-LIF separation, extremely concentrated buffers  
357 were needed (see section 3.1). In our first attempts, the BGEs having IS less than 100 mM  
358 were unable to create a sharp EOF transition for efficient preconcentration-separation of  
359 oligosaccharides. Much higher IS (150 mM or higher) were required to maintain the drastic  
360 change of  $\mu_{\text{EO}}$  between the two steps.

361 Finally, the new preconcentration approach was performed with the TEOA/Cit BGE (IS 200  
362 mM). Fig. 5 compares the LVSS-CE-LIF and the CE-LIF method without preconcentration  
363 for MD ladders. The monitoring of the current profile during the preconcentration (Fig. S3 in  
364 the ESI) showed that the low IS sample matrix filled in the capillary (reflected by the current  
365 approaching 0  $\mu\text{A}$  at the beginning) was gradually replaced by the high IS zone of the BGE  
366 (as the current increased). The LVSS preconcentration apparently transitioned to the CE-LIF  
367 separation mode without operator intervention when the matrix was 100 % removed and the  
368 BGE completely filled the capillary (i.e., stable current was reached). Based on the peak  
369 heights and injected sample concentrations, a detection sensitivity improvement of 200 times  
370 was achieved with the inclusion of LVSS. Besides the contribution of preconcentration effect,

371 this signal enhancement also comes from the fact that the high BGE IS required for EOF  
372 elimination during electrophoresis can boost at the same time the sample stacking effect (as  
373 shown in Fig. 1A). This resulted in further improvement of peak shapes and detection  
374 sensitivity. As the EOF was manipulated through IS changes rather than pH, we could select  
375 the best pH conditions for the analytes during preconcentration and separation. The peak  
376 sharpness was a bit compromised for the late-migrating peaks in the LVSS-CE-LIF mode.  
377 Considering that these peaks resulted from the stacking of a sample volume equivalent to 100  
378 % of the capillary volume (compared to 1 % in the normal CE -LIF mode), this slight change  
379 in peak sharpness and resolutions was considered to be tolerable. It is worthy to note that the  
380 different degree of polymerization glucose oligomers behaved differently in terms of  
381 enrichment factor and resolution changes after LVSS-CE-LIF (see Fig. S4). The improvement  
382 of peak height was more pronounced for the smallest DPs, whereas the peak resolution  
383 decreased more for them (except for DP1 and DP2) after LVSS process. This was probably  
384 due to the different DP responses to the new BGE compositions and/or preconcentration  
385 process, as it was already observed in another approach for preconcentration and CE-LIF of  
386 MD ladders [21]. The triplicates of electropherograms and current profiles from LVSS-CE of  
387 MD ladders (Fig. S5 in the ESI) demonstrated good repeatability of this process, with  
388 calculated RSD values less than 5 % for peak areas and 0.3 % for migration times. The current  
389 profile was used to monitor the successful completion and repeatability of the LVSS-CE  
390 process.

391

### 392 **3.2.3. Analysis of N-glycans**

393 To evaluate the performance of the proposed approach with glycoprotein-derived  
394 oligosaccharides, the BGE composed of 200 mM TEOA/Cit was used for preconcentration  
395 and CE-LIF separation of APTS-labeled N-glycans released from human IgG using PNGase

396 F. Most of human IgG N-glycans are bi-antennary complex type with low sialylation (5-10  
397 %), highly core-fucosylated (> 92 %); and a small proportion contains a bisecting GlcNAc (11  
398 %) [45]. By referring to the similar peak patterns assigned for human IgG using CE-LIF with  
399 the commercial BGE [46, 47], we could assign the corresponding N-glycan structures to the  
400 major peaks with our new buffer (Fig. 6A). Other peak identifications could be gleaned from  
401 the reference profile provided elsewhere [47]. With the new LVSS-CE-LIF method (Fig. 6B),  
402 while the same major peaks were separated with little decrease in resolution, the detection  
403 sensitivity was drastically improved (by approximately 160 folds, based on peak height). This  
404 in principle would allow more glycans including even minor ones, which are not easily  
405 visualized using standard CE-LIF protocol without preconcentration, to be detected. This  
406 method can indeed be applied to other negatively charged analytes, with the conditions that  
407 their electrophoretic mobilities are smaller than the EO mobility during preconcentration and  
408 at the same time higher than the EO mobility during the separation step.

409

#### 410 **4. Conclusion**

411 In this study we demonstrate the successful development of a new approach for LVSS via  
412 EOF modulation without recourse to any capillary coating or polymer addition. EOF can be  
413 modulated in a wide range and quasi-totally suppressed just by changing the IS of the BGE.  
414 New BGE compositions for CE-LIF were accordingly developed and the best constituents of  
415 TEOA/Cit were explored to allow signal improvement (5-fold over conventional protocols)  
416 and realization of this new LVSS mode (allowing signal enhancement by 200 times). This  
417 preconcentration approach does not require any user's intervention for transition to the  
418 subsequent separation step of enriched target molecules. The new mode of LVSS-CE is  
419 simple and straightforward and can be implemented on any CE instrument. This opens  
420 different alternatives of EOF-assisted preconcentration in fused silica capillaries, which were

421 utilized until now mainly for neutrally coated capillaries. These were successfully applied for  
422 separation and detection of glycoprotein-derived N- glycans, potentially offering diagnosis  
423 options for glycan-related diseases. Further improvement of glycan signals could be possible  
424 in the future by combining the new BGEs with multiple-cycles of large volume sample  
425 stacking, which is a recently developed electrokinetic preconcentration strategy [37].  
426 Development of other modes of EOF-assisted preconcentration using these new BGE  
427 compositions, as well as their exploitations for sensitive and selective determination /  
428 characterization of biomolecules and nanometric entities with CE-LIF are envisaged.

429

430

#### 431 *Acknowledgements*

432 The authors are grateful for the financial support by the Agence Nationale de la Recherche  
433 (ANR, France) with the grant no. ANR-18-CE29-0005-01. Bin Yang gratefully  
434 acknowledgements the China scholarship council for funding her Ph.D. scholarship. We  
435 thank Dr. Gabor Jarvas (University of Debrecen, Hungary) for his help in glycan profile  
436 interpretation

437

438

439

440

441

442

443

444

445

446

447

448

449  
450  
451  
452  
453  
454  
455  
456  
457  
458  
459  
460  
461  
462  
463  
464  
465  
466  
467  
468  
469  
470  
471  
472  
473

**References**

[1] P. Zhang, S. Woen, T. Wang, B. Liau, S. Zhao, C. Chen, Y. Yang, Z. Song, M.R. Wormald, C. Yu, P.M. Rudd, Challenges of glycosylation analysis and control: an integrated approach to producing optimal and consistent therapeutic drugs, *Drug Discov. Today*, 21 (2016) 740-765.

[2] M.H. Hu, Y. Lan, A. Lu, X.X. Ma, L.J. Zhang, Glycan-based biomarkers for diagnosis of cancers and other diseases: Past, present, and future, in: L. Zhang (Ed.) *Prog. Mol. Biol. Transl. Sci.*, 2019, pp. 1-24.

[3] B. Cylwik, M. Naklicki, L. Chrostek, E. Gruszewska, Congenital disorders of glycosylation. Part I. Defects of protein N-glycosylation, *Acta Biochim. Pol.*, 60 (2013) 151-161.

[4] T. Hennet, J. Cabalzar, Congenital disorders of glycosylation: a concise chart of glycoalyx dysfunction, *Trends Biochem. Sci.*, 40 (2015) 377-384.

[5] A.P. Corfield, M. Berry, Glycan variation and evolution in the eukaryotes, *Trends Biochem. Sci.*, 40 (2015) 351-359.

[6] A. Barroso, E. Gimenez, F. Benavente, J. Barbosa, V. Sanz-Nebot, Classification of congenital disorders of glycosylation based on analysis of transferrin glycopeptides by capillary liquid chromatography-mass spectrometry, *Talanta*, 160 (2016) 614-623.

[7] A. Bruneel, S. Cholet, T. Tran-Maignan, T.D. Mai, F. Fenaille, CDG biochemical screening: where do we stand? , *BBA - General Subjects*, 1864 (2020) 129652.

[8] G.Y. Qing, J.Y. Yan, X.N. He, X.L. Li, X.M. Liang, Recent advances in hydrophilic interaction liquid interaction chromatography materials for glycopeptide enrichment and glycan separation, *TrAC Trends Anal. Chem.*, 124 (2020).

- 474 [9] M.J. Kailemia, G.G. Xu, M. Wong, Q.Y. Li, E. Goonatileke, F. Leon, C.B. Lebrilla,  
475 Recent Advances in the Mass Spectrometry Methods for Glycomics and Cancer, *Anal.*  
476 *Chem.*, 90 (2018) 208-224.
- 477 [10] A. Banazadeh, L. Veillon, K.M. Wooding, M. Zabet-moghaddam, Y. Mechref, Recent  
478 advances in mass spectrometric analysis of glycoproteins, *Electrophoresis*, 38 (2017)  
479 162-189.
- 480 [11] G. Lu, C.L. Crihfield, S. Gattu, L.M. Veltri, L.A. Holland, Capillary Electrophoresis  
481 Separations of Glycans, *Chem. Rev.*, 118 (2018) 7867-7885.
- 482 [12] V. Mantovani, F. Galeotti, F. Maccari, N. Volpi, Recent advances in capillary  
483 electrophoresis separation of monosaccharides, oligosaccharides, and polysaccharides,  
484 *Electrophoresis*, 39 (2018) 179-189.
- 485 [13] M. Alexovič, Y. Dotsikas, P. Bober, J. Sabo, Achievements in robotic automation of  
486 solvent extraction and related approaches for bioanalysis of pharmaceuticals, *J.*  
487 *Chromatogr. B*, 1092 (2018) 402-421.
- 488 [14] R.A. Evangelista, M.S. Liu, F.T.A. Chen, Characterization of 9-aminopyrene-1, 4, 6-  
489 trisulfonate derivatized sugars by capillary electrophoresis with laser-induced  
490 fluorescence detection, *Anal. Chem.*, 67 (1995) 2239-2245.
- 491 [15] L.R. Ruhaak, G. Zauner, C. Huhn, C. Bruggink, A.M. Deelder, M. Wuhrer, Glycan  
492 labeling strategies and their use in identification and quantification, *Anal. Bioanal.*  
493 *Chem.*, 397 (2010) 3457-3481.
- 494 [16] Sciex, Fast Glycan Labeling & Analysis: Sensitive CE-LIF Detection with Automated  
495 Glycan Identification, [https://sciex.com/events/fast-glycan-webinar-1017-andras-](https://sciex.com/events/fast-glycan-webinar-1017-andras-guttman)  
496 [guttman](https://sciex.com/events/fast-glycan-webinar-1017-andras-guttman), (2018).

- 497 [17] Agilent, CE-LIF glycans,  
498 <https://www.agilent.com/cs/library/slidepresentation/public/Agilent->  
499 [Picometrics%20CE-LIF%20solution.pdf](https://www.agilent.com/cs/library/slidepresentation/public/Agilent-Picometrics%20CE-LIF%20solution.pdf), (2018).
- 500 [18] J. Sudor, M.V. Novotny, End-Label, Free-Solution Capillary Electrophoresis of Highly  
501 Charged Oligosaccharides, *Anal. Chem.*, 67 (1995) 4205-4209.
- 502 [19] F. Lamari, N.K. Karamanos, High performance capillary electrophoresis as a powerful  
503 analytical tool of glycoconjugates, *J. Liq. Chromatogr. Relat.*, 22 (1999) 1295-1317.
- 504 [20] Z. ElRassi, Y. Mechref, Recent advances in capillary electrophoresis of carbohydrates,  
505 *Electrophoresis*, 17 (1996) 275-301.
- 506 [21] H. Shao, B. Reider, G. Jarvas, A. Guttman, Z. Jiang, N.T. Tran, M. Taverna, On-line  
507 enrichment of N-glycans by immobilized metal-affinity monolith for capillary  
508 electrophoresis analysis, *Anal. Chim. Acta*, 1134 (2020) 1-9.
- 509 [22] B. Reider, M. Szigeti, A. Guttman, Evaporative fluorophore labeling of carbohydrates via  
510 reductive amination, *Talanta*, 185 (2018) 365-369.
- 511 [23] C. Varadi, C. Lew, A. Guttman, Rapid Magnetic Bead Based Sample Preparation for  
512 Automated and High Throughput N-Glycan Analysis of Therapeutic Antibodies, *Anal.*  
513 *Chem.*, 86 (2014) 5682-5687.
- 514 [24] S. Yang, H. Zhang, Solid-phase glycan isolation for glycomics analysis, *Proteomics Clin.*  
515 *Appl.*, 6 (2012) 596-608.
- 516 [25] Z. Szabo, A. Guttman, T. Rejtar, B.L. Karger, Improved sample preparation method for  
517 glycan analysis of glycoproteins by CE-LIF and CE-MS, *Electrophoresis*, 31 (2010)  
518 1389-1395.
- 519 [26] T. Kawai, N. Ota, A. Imasato, Y. Shirasaki, K. Otsuka, Y. Tanaka, Profiling of N-linked  
520 glycans from 100 cells by capillary electrophoresis with large-volume dual

- 521           preconcentration by isotachopheresis and stacking, *J. Chromatogr. A*, 1565 (2018) 138-  
522           144.
- 523 [27] E. Fukushima, Y. Yagi, S. Yamamoto, Y. Nakatani, K. Kakehi, T. Hayakawa, S. Suzuki,  
524           Partial filling affinity capillary electrophoresis using large-volume sample stacking with  
525           an electroosmotic flow pump for sensitive profiling of glycoprotein-derived  
526           oligosaccharides, *J. Chromatogr. A*, 1246 (2012) 84-89.
- 527 [28] T. Kawai, M. Ueda, Y. Fukushima, K. Sueyoshi, F. Kitagawa, K. Otsuka, Toward 10  
528           000-fold sensitivity improvement of oligosaccharides in capillary electrophoresis using  
529           large-volume sample stacking with an electroosmotic flow pump combined with field-  
530           amplified sample injection, *Electrophoresis*, 34 (2013) 2303-2310.
- 531 [29] T. Kawai, M. Watanabe, K. Sueyoshi, F. Kitagawa, K. Otsuka, Highly sensitive  
532           oligosaccharide analysis in capillary electrophoresis using large-volume sample stacking  
533           with an electroosmotic flow pump, *J. Chromatogr. A*, 1232 (2012) 52-58.
- 534 [30] Phoebus,  
535           [http://5.189.177.170/~analisis/site/objects/media/0/0/5/0/9/0050933\\_media/media1.pdf](http://5.189.177.170/~analisis/site/objects/media/0/0/5/0/9/0050933_media/media1.pdf).
- 536 [31] P. Kuban, P.C. Hauser, Ten years of axial capacitively coupled contactless conductivity  
537           detection for CZE - a review, *Electrophoresis*, 30 (2009) 176-188.
- 538 [32] A.J. Zemann, Conductivity detection in capillary electrophoresis, *TrAC Trends Anal.*  
539           *Chem.*, 20 (2001) 346-354.
- 540 [33] B.B. VanOrman, G.G. Liversidge, G.L. McIntire, T.M. Olefirowicz, A.G. Ewing, Effects  
541           of buffer composition on electroosmotic flow in capillary electrophoresis, *J.*  
542           *Microcolumn Separations*, 2 (1990) 176-180.
- 543 [34] J.C. Reijenga, T. Verheggen, J. Martens, F.M. Everaerts, Buffer capacity, ionic strength  
544           and heat dissipation in capillary electrophoresis, *J. Chromatogr. A*, 744 (1996) 147-153.

- 545 [35] P. Kubáň, P.C. Hauser, 20th anniversary of axial capacitively coupled contactless  
546 conductivity detection in capillary electrophoresis, *TrAC Trends Anal. Chem.*, 102  
547 (2018) 311-321.
- 548 [36] B.A. Williams, C. Vigh, Fast, accurate mobility determination method for capillary  
549 electrophoresis, *Anal. Chem.*, 68 (1996) 1174-1180.
- 550 [37] C.C. de Lassichere, T.D. Mai, M. Otto, M. Taverna, Online Preconcentration in  
551 Capillaries by Multiple Large-Volume Sample Stacking: An Alternative to  
552 Immunoassays for Quantification of Amyloid Beta Peptides Biomarkers in  
553 Cerebrospinal Fluid, *Anal. Chem.*, 90 (2018) 2555-2563.
- 554 [38] T.D. Mai, F. d'Orlye, A. Varenne, A Comprehensive Study of Silanization and Co-  
555 Condensation for Straightforward Single-Step Covalent Neutral Capillary Coating,  
556 *Chromatographia*, 78 (2015) 775-783.
- 557 [39] F. Kohlrausch, Ueber Concentrations-Verschiebungen durch Electrolyse im Inneren von  
558 Lösungen und Lösungsgemischen, *Ann. Phys. Chem.* , 298 (1897) 209-239.
- 559 [40] V. Hruška, B. Gaš, Kohlrausch regulating function and other conservation laws in  
560 electrophoresis, *Electrophoresis*, 28 (2007) 3-14.
- 561 [41] A. Kamgar, A. Bakhtyari, S. Mohsenpour, C. D'Agostino, G.D. Moggridge, M.R.  
562 Rahimpour, Mutual diffusion in concentrated liquid solutions: A new model based on  
563 cluster theory, *J. Mol. Liq.*, 232 (2017) 516-521.
- 564 [42] D. Corradini, G. Cannarsa, E. Fabbri, C. Corradini, Effects of alkylamines on  
565 electroosmotic flow and protein migration behaviour in capillary electrophoresis, *J.*  
566 *Chromatogr. A*, 709 (1995) 127-134.
- 567 [43] A. Bruneel, S. Cholet, V. Drouin-Garraud, M.L. Jacquemont, A. Cano, A. Megarbane, C.  
568 Ruel, D. Cheillan, T. Dupre, S. Vuillaumier-Barrot, N. Seta, F. Fenaille,  
569 Complementarity of electrophoretic, mass spectrometric, and gene sequencing

570 techniques for the diagnosis and characterization of congenital disorders of  
571 glycosylation, *Electrophoresis*, 39 (2018) 3123-3132.

572 [44] F. Kitagawa, T. Kawai, K. Otsuka, On-line sample preconcentration by large-volume  
573 sample stacking with an electroosmotic flow pump (LVSEP) in microscale  
574 electrophoresis, *Anal Sci*, 29 (2013) 1129-1139.

575 [45] J.N. Arnold, M.R. Wormald, R.B. Sim, P.M. Rudd, R.A. Dwek, The Impact of  
576 Glycosylation on the Biological Function and Structure of Human Immunoglobulins,  
577 *Annu. Rev. Immunol.*, 25 (2007) 21-50.

578 [46] G. Lu, L.A. Holland, Profiling the N-Glycan Composition of IgG with Lectins and  
579 Capillary Nanogel Electrophoresis, *Anal. Chem.*, 91 (2019) 1375-1383.

580 [47] A. Guttman, M. Szigeti, A. Lou, M. Gutierrez, Fast Glycan Labeling and Analysis :  
581 High-Resolution Separation and Identification in Minutes,  
582 [https://www.sciex.com/products/consumables/fast-glycan-analysis-and-labeling-for-the-](https://www.sciex.com/products/consumables/fast-glycan-analysis-and-labeling-for-the-pa-800-plus)  
583 [pa-800-plus](https://www.sciex.com/products/consumables/fast-glycan-analysis-and-labeling-for-the-pa-800-plus), (2018).

584

585

586

587

588

589

590

591

592

593

594

595

596

597

598

599

600

601

602

603

604

605 **Table captions:**

606 **Table 1.** List of BGE compositions at ionic strength of 150 mM and pH of 4.75, as simulated  
607 with Phoebus program for a use in a fused silica capillary of 50 $\mu$ m i.d. x 65cm length. The  
608 currents were calculated by the Phoebus program for the pre-defined voltage of 30 kV.

609

610

611 **Table 2:** Comparison of the salient data obtained with different BGEs for CE-LIF of  
612 oligosacharides, using uncoated fused silica capillaries (50  $\mu$ m I.D., 65 cm total length)

613

614

615

616

617

618

619

620

621

622

623

624

625

626

627

628 **Figure captions:**

629 Fig. 1. A) Working principle of the novel BGEs for CE-LIF of oligosaccharides. The ionic  
630 strengths (IS) of the BGE composed of large weakly charged molecules are increased  
631 to extremely high levels to allow high stacking of target analytes and at the same time  
632 suppression of EOF without recourse to any capillary coating. Oligosaccharides can be  
633 prepared in water or diluted BGE.

634 B) Principle of large volume sample stacking with EOF modulation and suppression in  
635 an uncoated fused silica capillary used in this study. This mode allows two completely  
636 different EOF magnitudes (via variation of the IS of the BGE) for sample  
637 preconcentration and for the separation of the stacked analytes.

638

639 Fig. 2. CE-LIF of oligosaccharides using different BGE compositions at pH 4.75. **A)** LiOH /  
640 AcOH IS of 25 mM (LiOH 25mM + AcOH 47 mM); **B)**  $\beta$ -Ala / Trimellitic acid IS of  
641 150 mM ( $\beta$ -Ala 1052 mM and Trimellitic acid 30 mM); **C)**  $\beta$ -Ala / AcOH IS of 150  
642 mM ( $\beta$ -Ala 861 mM and AcOH 127 mM) ; **D)** TEOA / AcOH IS of 150 mM (TEOA  
643 150 mM and AcOH 266 mM); **E)** TEOA / Cit IS of 150 mM (TEOA 150 mM and Cit  
644 58 mM). *F* denotes for residual fluorescent peaks. CE conditions: fused silica  
645 capillary, 50  $\mu$ m i.d., 50/60 cm, hydrodynamic injection at 50 mbar for 10 s, high  
646 voltage of -25 kV.

647

648 Fig. 3: CE-LIF of oligosaccharides using TEOA/Cit BGE at IS of **A)** 150 mM; **B)** 200 mM;  
649 **C)** Commercial Sciex BGE. *F* denotes for residual fluorescent peaks. CE conditions as  
650 in Fig. 2

651

652 Fig. 4 CE-LIF of N-glycans from human serum of healthy control and CDG individuals,  
653 using BGE composed of TEOA / Cit 200 mM in an uncoated silica capillary. A)  
654 Control patient, B) B4GALT1-CDG patient and C) MGAT2-CDG patient. Other CE  
655 conditions as in Fig. 2.

656

657 Fig. 5: CE-LIF with and without large volume sample stacking (LVSS) with EOF modulation  
658 of oligosaccharides, using BGE composed of TEOA/Cit at IS of 200 mM. A) LVSS-  
659 CE-LIF of oligosaccharides 200,000x dilution; **B)** CE-LIF of oligosaccharides 2000x  
660 dilution. Other conditions as in Fig. 2.

661

662 Fig. 6: **A)** CE-LIF of N-glycans released from human IgG; **B)** LVSS-CE-LIF of human IgG  
663 glycans using TEOA/Cit BGE at IS of 200 mM. Other CE conditions as in Fig. 2.

664

665

666

667

668

669

670

671

672

673

674

675

676

677

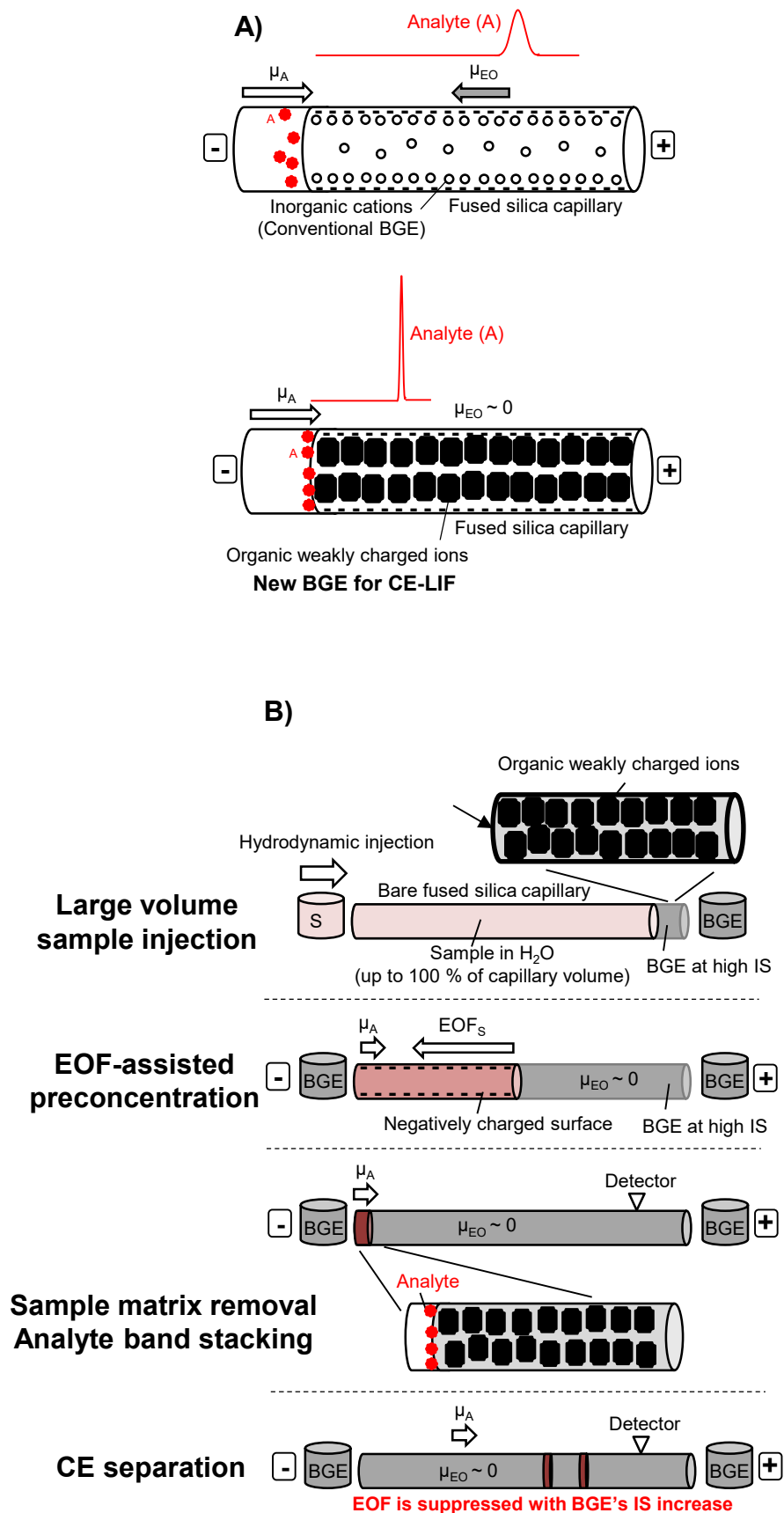
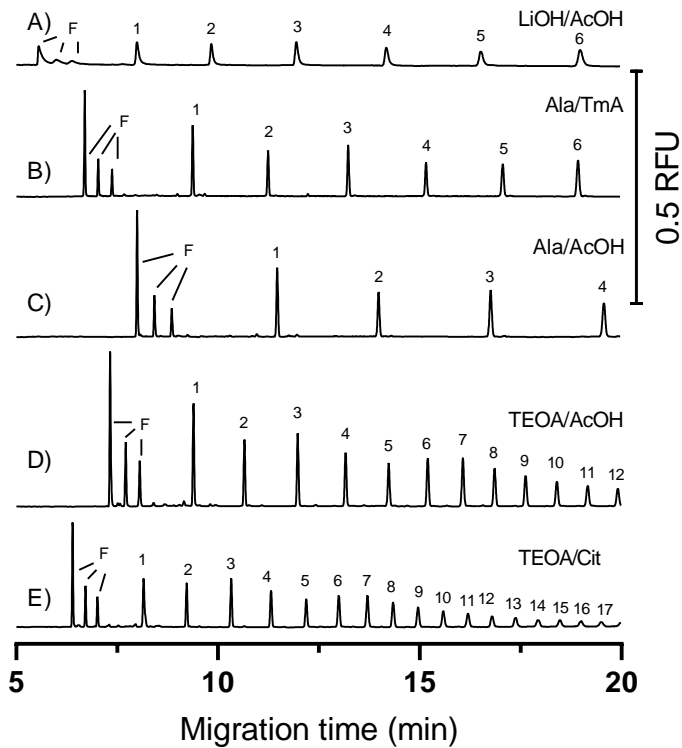
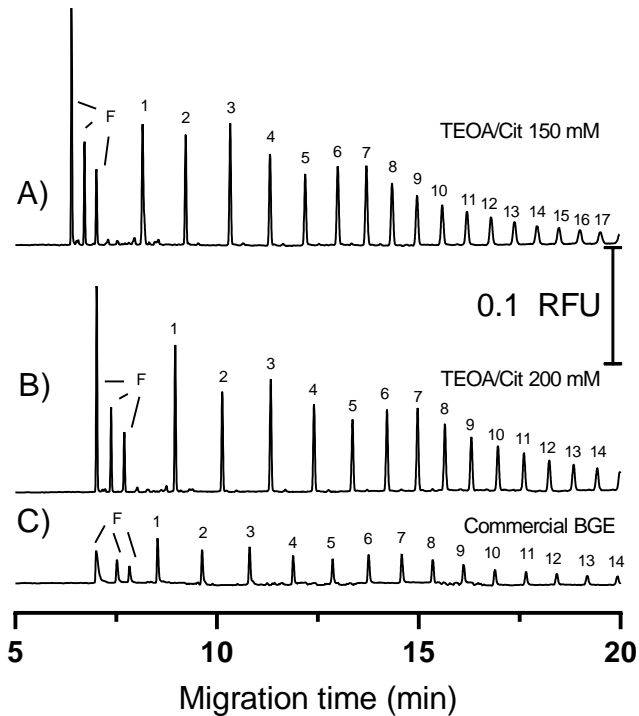


Figure 1



**Figure 2**



**Figure 3**

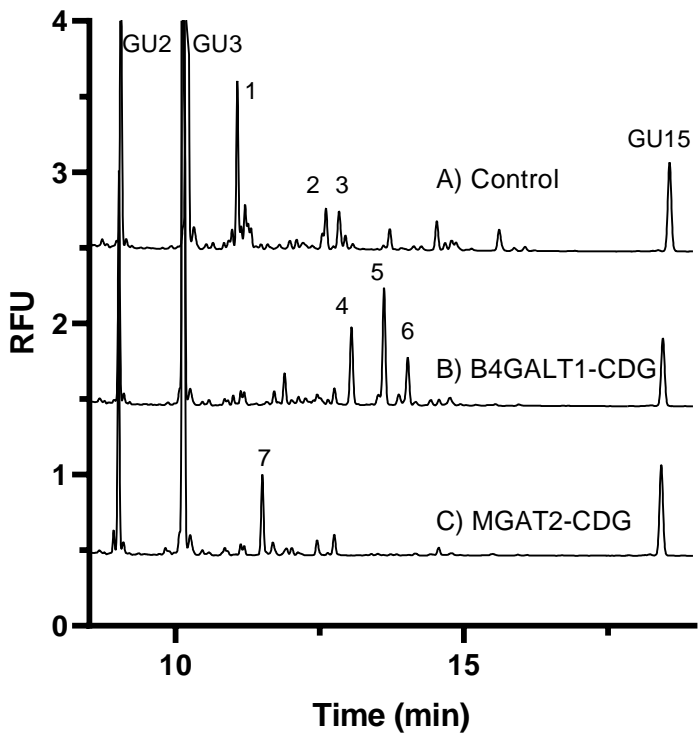


**Figure 4**

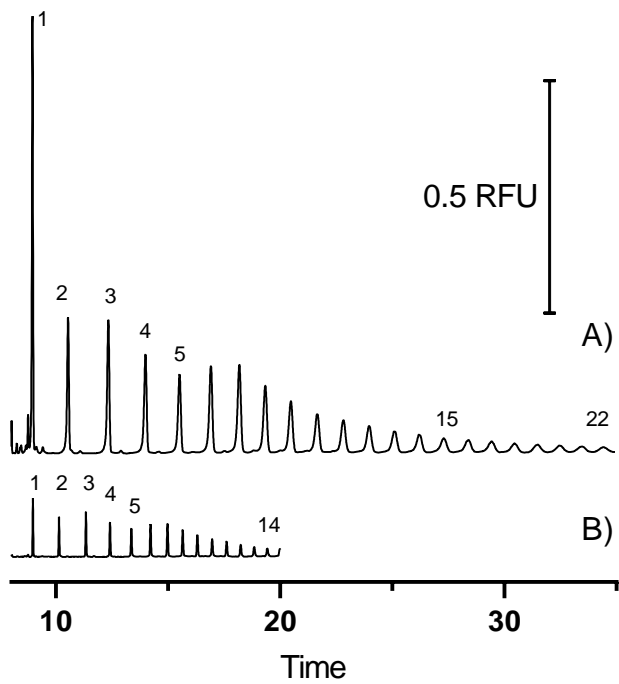


**Figure 5**

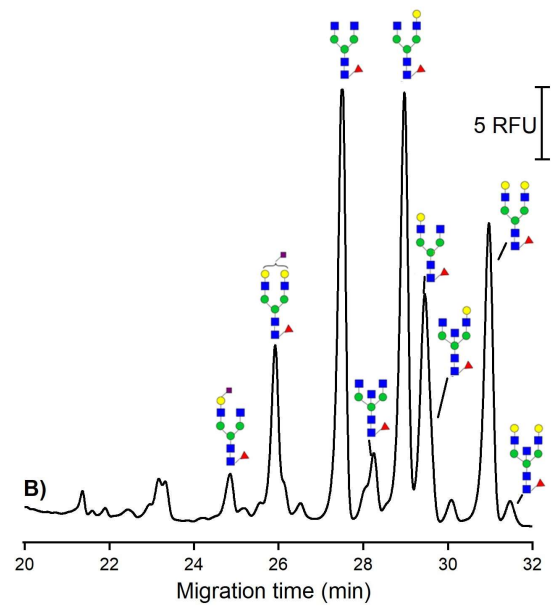
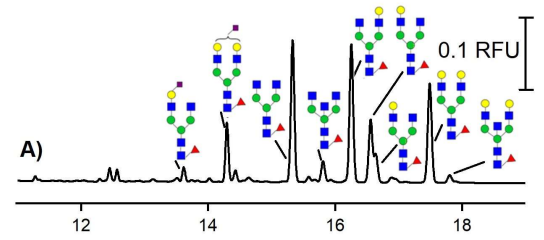


Figure 6

1 **Table 1.** List of BGE compositions at ionic strength of 150 mM and pH of 4.75, as simulated  
 2 with Phoebus program for a use in a fused silica capillary of 50 $\mu$ m i.d. x 60cm length. The  
 3 currents were calculated by the Phoebus program for the pre-defined voltage of 30 kV.

BGE compositions	I ( $\mu$ A) at 30kV	buffer capacity (mmol/l.pH)	Remark
LiOH 25mM + Acetic acid 47 mM (IS 25 mM)	16	28	Reference BGE
TEOA 150 mM + Acetic acid 266 mM (IS 150 mM)	21	155	Expected good quality
TEOA 150 mM + Citric acid 58 mM (IS 150 mM)	31	44	Expected good quality
$\beta$ -Ala 1052 mM + Trimellitic acid 30 mM (IS 140 mM)	19	185	Expected good quality
$\beta$ -Ala 963 mM + Acetic acid 127 mM (IS 70 mM)	57	506	High current generation
$\beta$ -Ala 861 mM + Pyromellitic Acid 19 mM (IS 150 mM)	16	152	Poor solubility of pyromellitic acid
TEOA 150 mM + Sorbic Acid 270 mM (IS 150 mM)	33	158	poor solubility of sorbic acid
TEOA 150 mM + Gluconic acid 160 mM (IS 150 mM)	27	20	poor solubility of gluconic acid
TEOA 150 mM + aspartic acid 166 mM (IS 150 mM)	31	34	poor solubility of aspartic acid
TEOA 150 mM + anisic acid 210 mM (IS 150 mM)	29	100	poor solubility of anisic acid
TEOA 150 mM + furoic acid 210 mM (IS 150 mM)	31	7	poor solubility of furonic acid

4

5

6 **Table 2:** Comparison of the salient data obtained with different BGEs for CE-LIF of  
 7 oligosaccharides, using uncoated fused silica capillaries (50  $\mu\text{m}$  i.d., 60 cm total length)

BGE compositions	Measured current ( $\mu\text{A}$ ) under HV of -25kV	The highest DP detected over a 20 min run	Signal / noise ratio for specific DP peaks		RSD % for migration time (n = 3)		RSD % for peak area (n = 3)	
			DP1	DP6	DP1	DP6	DP1	DP6
LiOH / AcOH 25 mM	14.5	6	64	48	0.92	0.30	1.37	2.46
$\beta$ -Ala / Trimel 140 mM	35	6	366	101	0.67	1.42	1.61	2.74
$\beta$ -Ala / AcOH 70 mM	70	4	414		0.83		0.46	
TEOA / AcOH 150 mM	53	12	646	149	0.28	0.42	1.51	0.59
TEOA / Cit 150 mM	51	17	659	260	0.26	0.21	4.46	1.06

8 \* DP: degree of polymerization of glucose oligomers

9